Origin of Second-Order Transverse Magnetic Anisotropy in Mn_{12}-Acetate

A. Cornia,[1] R. Sessoli,[2,*] L. Sorace,[2] D. Gatteschi,[2] A. L. Barra,[3] and C. Daiguebonne[4]

[1]*Dipartimento di Chimica and INSTM, Università di Modena e Reggio Emilia, via G. Campi 183, I-41100 Modena, Italy*
[2]*Dipartimento di Chimica and INSTM, Università di Firenze, Via della Lastruccia 3, I-50019, Sesto Fiorentino, Italy*
[3]*Grenoble High Magnetic Field Laboratory, MPI-FKF and CNRS, B.P. 166, F-38042 Grenoble Cedex 9, France*
[4]*Groupe de Recherche en Chimie et Métallurgie, INSA, F-35043 Rennes Cedex, France*

(Received 6 December 2001; published 27 November 2002)

The symmetry breaking effects for quantum tunneling of the magnetization in Mn_{12}-acetate, a molecular nanomagnet, represent an open problem. We present structural evidence that the disorder of the acetic acid of crystallization induces sizable distortion of the Mn(III) sites, giving rise to six different isomers. Four isomers have symmetry lower than tetragonal and a nonzero second-order transverse magnetic anisotropy, which has been evaluated using a ligand field approach. The result of the calculation leads to an improved simulation of electron paramagnetic resonance spectra and justifies the tunnel splitting distribution derived from the field sweep rate dependence of the hysteresis loops.

DOI: 10.1103/PhysRevLett.89.257201 PACS numbers: 75.45.+j, 31.15.Ct, 61.10.Nz

Molecules provide exciting opportunities for observing quantum phenomena in nanosize magnets [1–3]. The most investigated molecular compound is Mn_{12}-acetate, or Mn_{12}-Ac ($[Mn_{12}O_{12}(Ac)_{16}(H_2O)_4]\cdot 2HAc\cdot 4H_2O$, with HAc = acetic acid), a cluster with fourfold crystal symmetry comprising twelve Mn(III-IV) ions [4]. Understanding the physical properties of molecular compounds requires a detailed characterization of the structural features, which are rather different from those of extended lattices. We want to show in this Letter how x-ray diffraction techniques can help to unravel a problem related to the quantum tunneling of the magnetization in these systems.

Each Mn_{12}-Ac cluster is characterized by an $S = 10$ ground spin state experiencing a strong uniaxial anisotropy. Below 3 K the magnetization is frozen due to the energy barrier of ca. 60 K which hampers its reorientation [5]. The $S = 10$ ground state of the cluster is split into 21 sublevels describing a double-well potential according to the first term in the Hamiltonian

$$\mathbf{H} = D\mathbf{S}_z^2 - g_z\mu_B H_z \mathbf{S}_z, \tag{1}$$

which includes the axial anisotropy and Zeeman interaction with a magnetic field H_z directed along z. The quantum nature of the system is at the origin of the observation of steps in the hysteresis [1,2], which are observed whenever levels on opposite sides of the barrier have the same energy and tunneling below the barrier can occur. However, in order to observe tunneling the Hamiltonian must contain terms which do not commute with $\mathbf{S}_z$. A transverse magnetic field of any origin can induce tunneling, but in a zero or axially applied external field the dipolar or hyperfine fields are too weak to justify the observed tunneling rate. Second- and fourth-order transverse anisotropies described by the Hamiltonian

$$\mathbf{H}' = E(\mathbf{S}_x^2 - \mathbf{S}_y^2) + B/2(\mathbf{S}_+^4 + \mathbf{S}_-^4) \tag{2}$$

promote tunneling, the E term allowing transitions between states whose M, eigenvalue of $\mathbf{S}_z$, differ by multiples of two. However, the E parameter must vanish according to the fourfold crystal symmetry of the clusters. The symmetry-allowed fourth-order term in (2) permits tunneling every fourth step. However, all the transitions from $M = -10$ to $M' = 9, 8, \ldots$, etc., are experimentally observed on a similar footing. Several authors [6–9] have recently suggested the presence of symmetry breaking effects (i.e., a nonzero E parameter) in conjunction with a transverse magnetic field which activates odd transitions. The observed behavior has been justified assuming a broad Gaussian distribution of the E parameter. Among the possible physical origins of local symmetry lowering Chudnovsky *et al.* proposed crystal dislocations [10].

Now the detailed x-ray diffraction analysis at low temperature shows that most of the Mn_{12}-Ac molecules in the crystal do not actually possess fourfold symmetry [11]. In fact, the tetragonal symmetry is disrupted by the acetic acid molecules disordered over two sites around twofold axes. The anisotropy axis of a Mn(III) site is significantly bent when hydrogen-bond interaction with the acetic acid occurs. In principle, this gives rise to six different types of clusters, whose relative abundance can be calculated assuming statistical distribution. In the following we will present the structural evidence and then we will use a ligand field model to calculate the second-order anisotropy parameters D and E. Additional high field electron paramagnetic resonance (HF-EPR) evidences will be provided and the tunnel splitting will be calculated.

The $[Mn_{12}O_{12}(Ac)_{16}(H_2O)_4]$ clusters develop around S_4 axes of tetragonal space group $I\bar{4}$ and are consequently crystallographically axial (see Fig. 1). The lattice also comprises four water molecules and two acetic acid molecules, CH_3COOH(O14, O15, C9, C10), per cluster (for the atom labeling scheme see Fig. 2) not directly bound

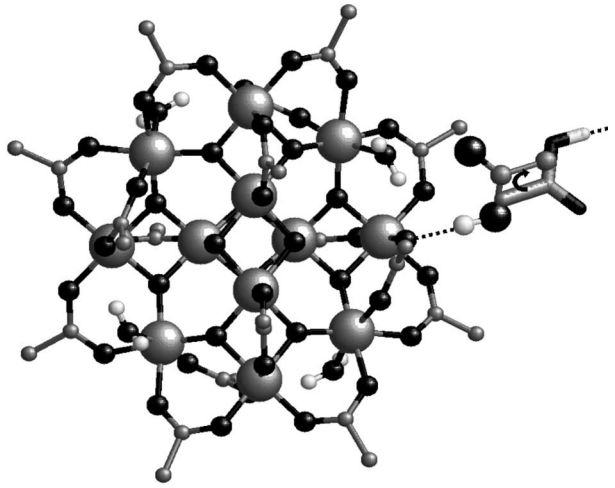

FIG. 1. Structure of the $[Mn_{12}O_{12}(CH_3COO)_{16}(H_2O)_4]$ cluster at 83 K viewed slightly off the S_4 axis. The manganese atoms are represented as large spheres, oxygens are black, carbons grey, and hydrogens white. The acetic acid is disordered on two positions related by a binary axis (curved arrow). For clarity only one of the four symmetry-related disordered sites is reported. When the acetic acid occupies the position evidenced by large spheres a hydrogen bond (dashed line) with the core of the cluster is formed. In the position evidenced by a thicker backbone the same bond is formed with the neighboring cluster.

to the Mn_{12} core. The latter are located around twofold axes between adjacent Mn_{12} units and are consequently disordered over two equally populated positions but are involved in a strong hydrogen-bonding interaction with the acetate ligand O6-O7-C3-C4 [11,12]. Interestingly, according to room-temperature x-ray data [4], C4 and O6 have unusually large Debye-Waller parameters (B_{eq} = 15.06 and 4.35 Å^2, respectively) as compared to corresponding atoms in the remaining acetate moieties (4.07–4.38 Å^2 for methyl carbon atoms and 2.19–3.25 Å^2 for oxygen atoms, respectively). Our analysis performed at 83 K confirms the disorder effects on the acetic acid molecule and the presence of a strong hydrogen bond between O15 and O6 [O15–O6=2.866(6) Å, O15–H15 $\cdots$ O6=174.6(3)°] as shown in Figs. 1 and 2 [11]. More importantly, we have found that the displacement ellipsoids of O6, C4, and, to a lesser extent, of O7 and C3 are abnormally elongated, pointing to the presence of disorder effects on the acetate ligand too (Fig. 2). An alternative structural model has then been used in which the acetate ligand is allowed to reside in two different positions (A and B). The validity of this model, which implies the absence of a broad distribution of positions, is confirmed by the fact that the Debye-Waller parameters of C4 and O6 are comparable to those of the other atoms. The best-fit occupancies are 0.46(1) and 0.54(1) for A and B, respectively. The values, close to 0.5, strongly suggest that the disorder of the acetate ligand results from the hydrogen-bond interaction with the disordered acetic acid molecules, which occupy half of the sites. The hydrogen

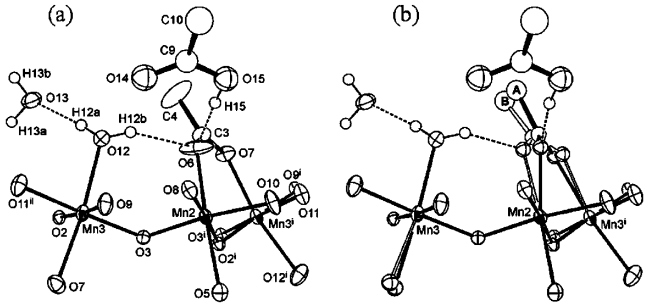

FIG. 2. Coordination sphere of Mn2 and Mn3, as determined from anisotropic refinement of the displacement factors of C3, C4, O6, and O7 (a) and from an isotropic model with disorder fitting (b). Thermal ellipsoids are at 50% probability level. Methyl hydrogen atoms are omitted for clarity.

bond, when present, leads to a sizable displacement of O6 toward O15 (Fig. 2).

In principle, each of the four symmetry-related acetate ligands derived from O6-O7-C3-C4 can be involved in H-bonding interactions of this type. Six different isomeric forms of Mn_{12}-Ac can thus be envisaged which differ in the number ($n = 0, 1, \ldots, 4$) and arrangement of hydrogen-bound acetate ligands (Fig. 3). Clearly, strict axial symmetry can be retained in the case of a regular pattern of $n = 0$ and $n = 4$ isomers. However, this would lead to a supercell with doubled lattice constants ($a' = b' = 2a$) for which no experimental evidence has been found. We conclude that the average molecular symmetry of Mn_{12}-Ac clusters is lower than axial.

The most important contribution to the magnetic anisotropy in Mn_{12}-Ac is expected to arise from the Jahn-Teller distorted Mn(III) sites. We have shown in a previous publication [13] that the magnetic anisotropy of Mn(III) ions can be predicted with a great accuracy by taking into account the crystal field generated by the ligands and introducing the real geometry of the coordination sphere using the angular overlap model (AOM) [14]. The encouraging results of a first attempt of rationalization of the zero-field splitting (ZFS) of Mn_{12}-Ac on the basis of AOM [15] have suggested that this approach might provide reasonable estimates of the magnetic anisotropy differences among the various isomers,

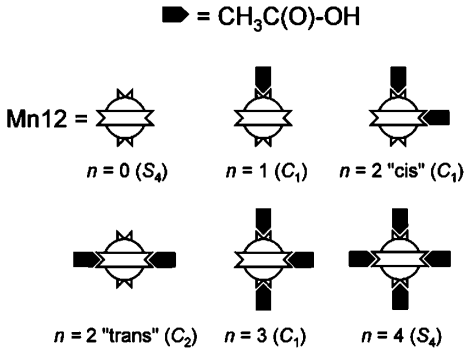

FIG. 3. The six isomers of Mn_{12}-Ac as discussed in the text.

TABLE I. Calculated Mn(III) magnetic anisotropy parameters.[a]

Site	D (K)	E (K)	δ (°)[b]
Mn2A	−4.92	0.40	11.6
Mn2B	−5.27	0.27	10.7
Mn3A	−4.57	0.10	37.2
Mn3B	−4.40	0.07	37.1

[a]Racah parameters equal to the free ion values are assumed with an orbital reduction factor $k = 0.75$.
[b]δ is the angle between the easy-axis direction of each manganese site and the crystallographic c axis.

eventually elucidating features of the low-temperature spin dynamics. Because of disorder effects, four different coordination geometries must be considered for the Mn(III) ions, namely, two for Mn2 and two for Mn3 (see Fig. 2). Mn(IV) sites were neglected given the small expected contribution to the global ZFS. The values of the AOM parameters for each donor atom, taken from literature data, have been corrected for the actual metal-ligand distance assuming an exponential dependence. The angular coordinates are obtained from the centroids of the thermal ellipsoids of the structure determination, while the D and E parameters are calculated as described elsewhere [14].

In Table I we report the results obtained from the calculation. As can be seen, the interaction with the acetic acid molecule induces only minor changes in the D and E parameters as well as in the direction of the easy axis. In order to evaluate the departure from tetragonal symmetry we have calculated the projection of the single-ion contribution on the $S = 10$ ground spin state. Using the coupling scheme described in [16] the projection coefficient is identical for all the Mn(III) ions ($d_2 = d_3 = 0.02845$). The total anisotropy tensor for each of the six species shown in Fig. 3 has been then calculated by performing the summation

$$\mathbf{D}_{\text{tot}} = d_2 \sum_{i=1}^{4} \mathbf{R}_i^T \mathbf{D}_2^{\alpha(i)} \mathbf{R}_i + d_3 \sum_{i=1}^{4} \mathbf{R}_i^T \mathbf{D}_3^{\alpha(i)} \mathbf{R}_i, \qquad (3)$$

where $\alpha(i) = A$ or B. In the above equation, $\mathbf{D}_2^{\alpha(i)}$ and $\mathbf{D}_3^{\alpha(i)}$ are the single-ion ZFS tensors for the Mn2 and Mn3 sites in the crystal reference frame, and $\mathbf{R}_i$ is the matrix representation of the ith symmetry operation of the S_4 point group. The resulting $\mathbf{D}_{\text{tot}}$ tensor turns out to be axial and diagonal in the crystal axes reference frame only for $n = 0$ and $n = 4$. In the other four cases nonzero off diagonal terms are present, and diagonalization of the matrices provided the D and E parameters along with the angle θ between the easy axis of a cluster and the crystallographic c axis (Table II). The agreement between the calculated D parameter and the experimental ones found by several techniques [17–19] is acceptable considering the approximations involved. The D parameter is equal for all the species within $\pm 2\%$ and the easy-axis direction does not deviate significantly from the crystallographic c axis ($<0.5°$). The relative abundance of the various species has been calculated assuming an equal probability of sites A and B, in agreement with the experimentally determined occupancies, which are very close to $1/2$.

HF-EPR is in principle sensitive to the presence of transverse anisotropy in the cluster. Figure 4 shows the high field region of the experimental polycrystalline powder spectra recorded at $T = 35$ K with the exciting frequency of 525 GHz [17]. The simulation has been obtained by using the second- and fourth-order axial parameters as in [17] taking into account the relative deviation from the average D parameter and the distribution of second-order transverse terms as indicated in Table II. Only B has been left free to vary and a good simulation has been obtained only for $B \neq 0$. The spectra of Fig. 4 have been calculated with $B = 4 \times 10^{-5}$ K, very close to that derived by inelastic neutron scattering experiments [18]. The agreement with the experimental data improves significantly compared to the previous simulation where only the fourth-order transverse term was considered [17].

The single crystal spectrum at 5 K and 95 GHz recorded with the field at 30° from the a crystallographic axis in the ab plane (inset of Fig. 4) shows a complex structure of peaks, which is clearly incompatible with strict tetragonal symmetry. The 30° spectrum has been chosen because for this angle we expect the maximum sensitivity to the E parameter for all nonaxial species. In fact the hard axes of the nonaxial clusters are pointing

TABLE II. Calculated magnetic anisotropy and tunnel splitting of the isomers of Mn_{12}-Ac.

Isomer	Concentration	D (K)	E (K)	θ (°)	$\Delta_{-10,4}$ (K)[a]
$n = 0$	6.25%	−0.759	0	0	0
$n = 4$	6.25%	−0.797	0	0	0
$n = 1$	25%	−0.769	2.34×10^{-3}	0.3	8.8×10^{-8}
$n = 2$ cis	25%	−0.778	1.87×10^{-4}	0.4	7.0×10^{-9}
$n = 2$ trans	12.5%	−0.778	4.70×10^{-3}	0	1.7×10^{-7}
$n = 3$	25%	−0.788	2.35×10^{-3}	0.3	8.9×10^{-8}

[a]The spin Hamiltonian parameters are the same as in [18] where the E term reported in the 4th column has been added.

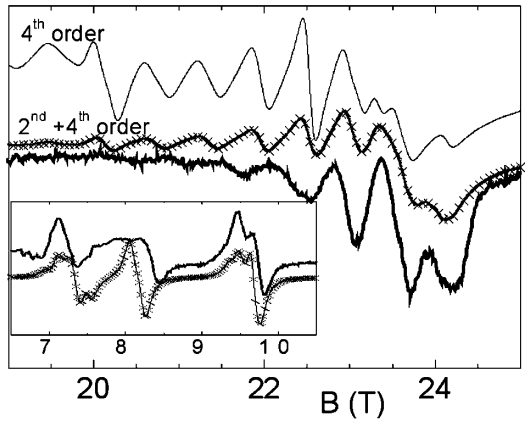

FIG. 4. HF-EPR spectra of a polycrystalline sample of Mn_{12}-Ac at 35 K and 525 GHz (bold line), simulation obtained in [17] (thin line), and in this work (line with crosses). In the inset experimental (bold line) and simulated (line with crosses) single crystal spectrum at 95 GHz and 5 K with the magnetic field at 30° from a in the ab plane.

toward different directions, and the simulation reported in Fig. 4 has also considered the four tetragonally related orientations of the anisotropy tensors. The agreement is acceptable considering the limited number of adjustable parameters. A best-fit simulation of the single crystal spectra and a critical evaluation of the many parameters involved in the simulation is left for a separate publication.

The presence of a distribution of magnetic anisotropy in crystals of Mn_{12}-Ac has also been experimentally evidenced by a detailed study of the dependence of the steps in the hysteresis loops on the field sweeping rate [6–8]. The ground state tunnel splitting $\Delta_{\pm 10}$ is practically unaffected by such small values of E but this is not the case for resonances occurring at higher fields.

To compare our study with the experimental results in [6] we have evaluated the tunnel splitting induced by the presence of the second-order magnetic anisotropy for the transition between the $M = -10$ and $M' = 4$ state. In Table II we report the tunnel splitting for this transition calculated by exact diagonalization of the Hamiltonian matrix, assuming the other parameters of the spin Hamiltonian as in [18]. The $\Delta_{-10,4}$ for such a transition is zero for species $n = 0$ and $n = 4$, in agreement with their higher symmetry, and varies between 7.0×10^{-9} K and 1.7×10^{-7} K for the others. These values are in good agreement with the center of the distribution of tunnel splitting, $\Delta_{-10,4} \approx 3 \times 10^{-8}$ K, used in [6] to scale the experimental data, and also with the width of the tunnel distribution reported recently in [7]. If our calculation is repeated by neglecting B the calculated splitting is several orders of magnitude smaller, as the E term is much less efficient in promoting tunneling between states with large $|M|$. The coexistence of both terms is in agreement with the EPR analysis as well as with other experimental evidences [18–20]. Tunneling at odd transitions is of course not accounted for by this model and requires the presence of a transverse field of dipolar or hyperfine origin.

In conclusion we have provided unambiguous experimental evidence that most Mn_{12}-Ac molecules experience a symmetry lower than tetragonal. The order of magnitude of the quadratic anisotropy has been determined and found to be distributed around discrete values, which are in agreement with the distribution used to justify experimental results on the dynamics of the magnetization [6]. Our results show that the magnetocrystalline anisotropy is only slightly affected by perturbations of the crystal structure involving the metal coordination. In this soft molecular crystal, it seems therefore quite unreasonable that dislocations could induce substantial modification of the magnetic anisotropy at long distance as proposed in [10]. Dislocations and small deviations of the atomic positions from the centroids of the thermal ellipsoids can be a source of distribution in the magnetic anisotropy but the acetic acid of crystallization is the main source of the different magnetic anisotropy, and consequently tunnel splitting, experienced by the molecules.

We are indebted to T. Roisnel for his assistance in the low-temperature x-ray data collection. The financial support of Italian MIUR and CNR and of the EC(HPRN-CT-1999-0012) is acknowledged.

*Corresponding author.
Email address: roberta.sessoli@unifi.it

[1] J. R. Friedman *et al.*, Phys. Rev. Lett. **76**, 3830 (1996).
[2] L. Thomas *et al.*, Nature (London) **383**, 145 (1996).
[3] D. Loss and M. N. Leuenberger, Nature (London) **410**, 789 (2001).
[4] T. Lis, Acta Crystallogr. Sect. B **36**, 2042 (1980).
[5] R. Sessoli *et al.*, Nature (London) **365**, 141 (1993).
[6] K. M. Mertes *et al.*, Phys. Rev. Lett. **87**, 227205 (2001).
[7] E. del Barco *et al.*, cond-mat/0209167 [Europhys. Lett. (to be published)].
[8] R. Amigo *et al.*, Phys. Rev. B **65**, 172403 (2002).
[9] B. Parks *et al.*, Phys. Rev. B **64**, 184426 (2001).
[10] E. M. Chudnovsky and D. A. Garanin, Phys. Rev. Lett. **87**, 187203 (2001).
[11] A. Cornia *et al.*, Acta Crystallogr. Sect. C **58**, 371 (2002).
[12] P. Langan *et al.*, Acta Crystallogr. Sect. C **57**, 909 (2001).
[13] A. L. Barra *et al.*, Angew. Chem., Int. Ed. Engl. **36**, 2329 (1997).
[14] A. Bencini, I. Ciofini, and M. G. Uytterhoeven, Inorg. Chim. Acta **274**, 90 (1998).
[15] D. Gatteschi and L. Sorace, J. Solid State Chem. **159**, 253 (2001).
[16] F. Hartmann-Boutron, P. Politi, and J. Villain, Int. J. Mod. Phys. B **10**, 2577 (1996).
[17] A. L. Barra, D. Gatteschi, and R. Sessoli, Phys. Rev. B **56**, 8192 (1997).
[18] I. Mirebeau *et al.*, Phys. Rev. Lett. **83**, 628 (1999).
[19] A. Cornia *et al.*, Chem. Phys. Lett. **322**, 477 (2000).
[20] S. Hill *et al.*, Phys. Rev. Lett. **80**, 2453 (1998).